Sequential disruption of the shortest path in critical percolation

Oliver Gschwend[1,*] and Hans J. Herrmann[2,3]
[1]*ETH Zürich, Computational Physics for Engineering Materials, Institute for Building Materials, Wolfgang-Pauli-Str. 27, HIT, CH-8093 Zürich, Switzerland*
[2]*Departamento de Física, Universidade do Ceará, 60451-970 Fortaleza, Brazil*
[3]*ESPCI, CNRS UMR 7636–Laboratoire PMMH, 75005 Paris, France*

(Received 16 June 2019; published 16 September 2019)

We investigate the effect of sequentially disrupting the shortest path of percolation clusters at criticality by comparing it with the shortest alternative path. We measure the difference in length and the enclosed area between the two paths. The sequential approach allows us to study spatial correlations. We find the lengths of the segments of successively constant differences in length to be uncorrelated. Simultaneously, we study the distance between red bonds. We find the probability distributions for the enclosed areas A, the differences in length Δl, and the lengths between the red bonds l_r to follow power-law distributions. Using maximum likelihood estimation and extrapolation we find the exponents $\beta = 1.38 \pm 0.03$ for Δl, $\alpha = 1.186 \pm 0.008$ for A, and $\delta = 1.64 \pm 0.03$ for the distribution of l_r.

DOI: 10.1103/PhysRevE.100.032121

I. INTRODUCTION

The optimum path through a random energy landscape has been studied exhaustively in the past [1–4]. In particular also the blocking of sites along the optimum path and the resulting second best path has been considered [5]. Percolation clusters at criticality are realizations of fractal uncorrelated random landscapes and in the present paper we will study blocking the shortest path. We consider site percolation on a square lattice at the critical threshold. Assuming the model describes a traffic situation [6] or a forest fire [7], it is important to know how far the bypass and the surrounded area will be in case of a blockade in the shortest path. A similar investigation to ours was performed before [8] but on a directed bond percolation grid and without the sequential approach which allows to obtain the spatial correlations along the path. Nevertheless, due to strong analogies between the two models [9], we expect to obtain similar results.

II. MODEL

We simulate site percolation on a two-dimensional square lattice at the percolation threshold $p_c = 0.592746$ [10]. In the horizontal direction (left, right) we choose periodic boundary conditions to reduce finite-size effects. In the vertical direction the upper and the lower boundaries are open. Using the burning algorithm [11], we first extract the shortest path l, or "chemical distance" [12], between the upper and the lower border of the lattice, which is known to be fractal at $p = p_c$ [11,13–16]. In our case we consider only systems in which two completely separated shortest paths (paths that have no sites in common) do not exist. In the case where the shortest path is not unique, e.g., contains two or more alternative routes of equal length, we randomly choose one. Next, we walk along the shortest path, sequentially blocking each time one site on the path and then run the burning algorithm again to find the shortest alternative path. If there are several second shortest paths of equal length, then we choose the one enclosing the smallest area with the original one. After each blocking event, the blocked site will be unblocked again. An example is shown in Fig. 1, where the original shortest path (yellow dotted) is blocked (red square) and the shortest alternative path is found (blue dashed). The enclosed area is filled in light blue and the difference in length is obtained by subtracting the lengths of the two paths. In order to obtain good statistics we perform at least 1.4 million blocking events per lattice size, which ranges from $L = 200$ to $L = 15\,000$. We choose the functional form of the probability density function by comparing the log-likelihood ratios from lognormal, exponential, power law, and exponentially truncated power law and exclude the risk of overfitting by verifying our form by calculating the Akaike information criterion according to Ref. [17]. According to Ref. [18], we use maximum likelihood estimation (MLE) for discrete exponentially truncated power laws based on the method used in Ref. [19]. The estimated exponents for different lattice sizes L show algebraic convergence to some limit value γ_0 as $L \to \infty$. By fitting the estimated exponents $\gamma(L)$ against $\gamma(L) = \gamma_0 + \gamma_s L^{\gamma_e}$ using nonlinear least squares, we extrapolate γ_0. Since the probability distribution in Sec. IV (Fig. 4) follows a power law which is flattened in the beginning, we cannot use the method from Ref. [19]. Instead, we use a least-squares fit applied on 12 normalized log bins using the point numbers 3 to 11.

III. DISTANCES BETWEEN SUCCESSIVE RED BONDS

We start by extracting the shortest path and plotting the average length of the shortest paths $\langle l \rangle$ against the lattice size. We obtain the fractal dimension of the shortest path

*olivergschwend@gmx.ch

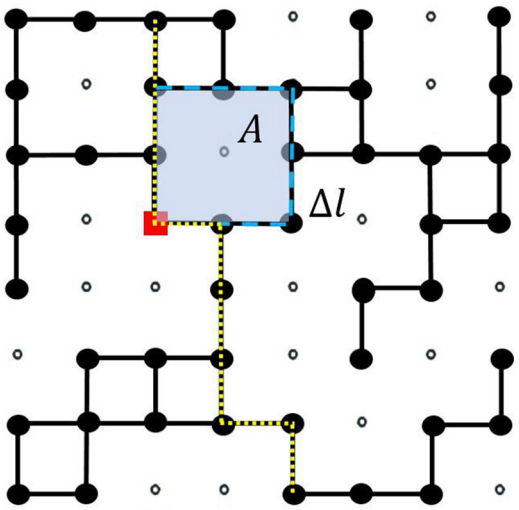

FIG. 1. A percolating cluster with the shortest path (yellow dotted line), a site from the shortest path blocked (red square), alternative second shortest path (blue dashed line), and the smallest enclosed area A (blue shaded area). Δl is the difference in length between the two paths, here $\Delta l = 2$.

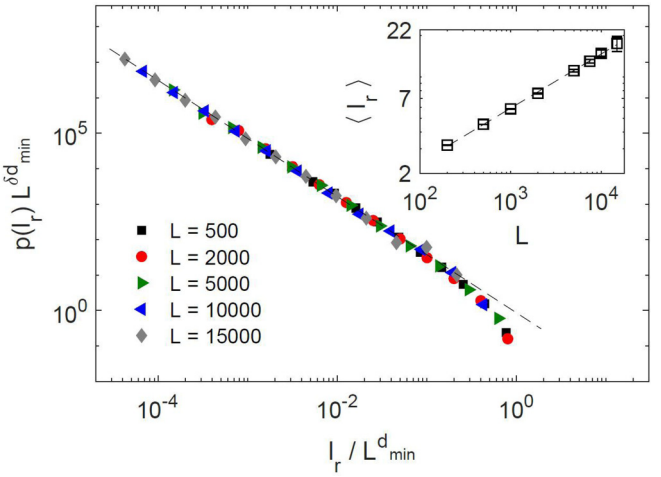

FIG. 2. Data collapse for the probability distribution function for the distances between red bonds $p(l_r)$ for different lattice sizes L. The dashed line represents a power-law fit with exponent $\delta = 1.64 \pm 0.03$. The inset shows the average length between red bonds $\langle l_r \rangle$ for different lattice sizes L. The dashed line is a power-law fit with exponent 0.39 ± 0.02 giving the lattice size dependency of $\langle l_r \rangle$.

$\langle l \rangle \sim L^{d_{\min}}$ with $d_{\min} = 1.123 \pm 0.015$, which is within the error bars in good agreement with Ref. [20].

Next we start blocking the shortest path at the topmost site on the upper border and wander along the shortest path until the lower border is reached. This process of blocking all sites in a successive order we call "sequential disruption". Each time we block a site, we look for the shortest alternative path through the lattice. In the case where no alternative path through the lattice exists, we are blocking a cutting or red bond [14]. A red bond is defined as a site belonging to the shortest path, which, when blocked, disrupts the whole connection from the top to the bottom. Supposing that the locations of the red bonds along the shortest path are uncorrelated [11], we propose that the average length between red bonds $\langle l_r \rangle$ scales as the ratio of the shortest path length $\langle l \rangle$ and the number of red bonds $\langle n_r \rangle$,

$$\langle l_r \rangle \sim \frac{\langle l \rangle}{\langle n_r \rangle} = L^{d_{\min} - \frac{1}{\nu}}, \tag{1}$$

because the number of red bonds scales with $\langle n_r \rangle \sim L^{\frac{1}{\nu}}$ [21], where $\nu = 4/3$ is the exponent of the divergence of the correlation length [22] and the shortest path scales with $\langle l \rangle \sim L^{d_{\min}}$, with $d_{\min} = 1.13077(2)$ [20]. As shown in the inset of Fig. 2, we find that $\langle l_r \rangle$ scales with L as $L^{0.39 \pm 0.02}$, which is within error-bar agreement with Eq. (1).

We also study their empirical probability distribution. We find the probability distribution of l_r to follow an exponentially truncated power law. We propose the following scaling ansatz:

$$p(l_r, L) = L^{-\delta d_{\min}} F\left(\frac{l_r}{L^{d_{\min}}}\right). \tag{2}$$

We divide the argument of the scaling function F by $L^{d_{\min}}$ motivated by the fact that l_r is naturally limited by the shortest path length. Using that the scaling function $F(x) \sim x^{-\delta}$ for $x \to \infty$, we have to multiply the scaling function with $L^{-\delta d_{\min}}$. We confirm our scaling ansatz with the good data collapse shown in Fig. 2 with the exponent $\delta = 1.64 \pm 0.03$. The truncation is due to the finite size of the systems and is expected to vanish for $L \to \infty$.

IV. DIFFERENCE IN LENGTH BETWEEN SHORTEST PATHS

In this section we discuss the results concerning the difference in length between the shortest path and the next shortest alternative after removing one site of the shortest path. We observe two cases of alternative paths. They can either have the same (convergent) or different (divergent) starting and end points. In the latter case the two paths together form an open fork toward the upper or lower border of the system. As shown in Fig. 3, we measure the fraction of each case. Using an algebraic fit of the form $f = f_0 + p_1 L^{p_2}$, where f_0 is the extrapolated value of the fractions for $L \to \infty$, we find that the fraction of divergent cases (red circles) tends to -0.01 ± 0.03 with the fitting parameters $p_1 = 1.47$ and $p_2 = -1.34$, which suggests that the divergent case might be just a finite-size effect and disappears in the infinite limit. It might also be that the fraction of divergent paths does go to a very small number in the thermodynamic limit [23,24]. Consequently, we include only the convergent case in further studies.

We find the probability distribution of Δl to follow an exponentially truncated power law. We propose the scaling ansatz of the form:

$$p(\Delta l, L) = L^{-\beta d_{\min}} G\left(\frac{\Delta l}{L^{d_{\min}}}\right). \tag{3}$$

The division of the argument of the scaling function G by $L^{d_{\min}}$ is motivated by the fact that the fractal dimension of shortest distance follows $\langle l \rangle \sim L^{d_{\min}}$ [20]. We find the best

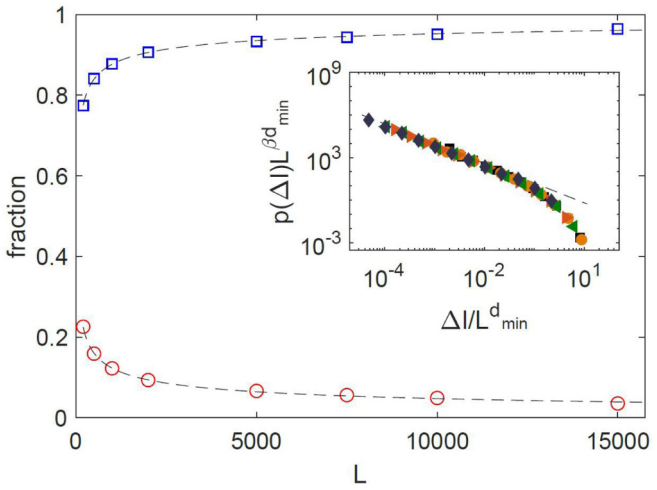

FIG. 3. The fraction of convergent (blue squares) and divergent (red circles) alternative paths. The dashed line represents the algebraic fit. The inset shows the data collapse for the probability distributions for the difference in length Δl for different lattice sizes, ranging from $L = 500$ to $L = 15\,000$. The dashed line depicts a power-law fit with exponent $\beta = 1.38 \pm 0.03$.

model to be an exponentially truncated power law. Indeed, we observe a convincing data collapse shown in the inset of Fig. 3 and hence confirm our proposed scaling ansatz with an estimated exponent of $\beta = 1.38 \pm 0.03$. This value is consistent with the one found on a randomly directed square lattice in Ref. [8], where an exponent of 1.36 ± 0.01 was reported.

We now consider the spatial correlation of the detours. Therefore, we walk along the shortest path and count over how many blocked sites the difference in length Δl between the shortest path and the next shortest path stays the same. Successive sites which show the same difference in length belong to the same "segment". As an example, consider in Fig. 1, instead of the red indicated site, the previous one being blocked. Both the alternative path and the difference

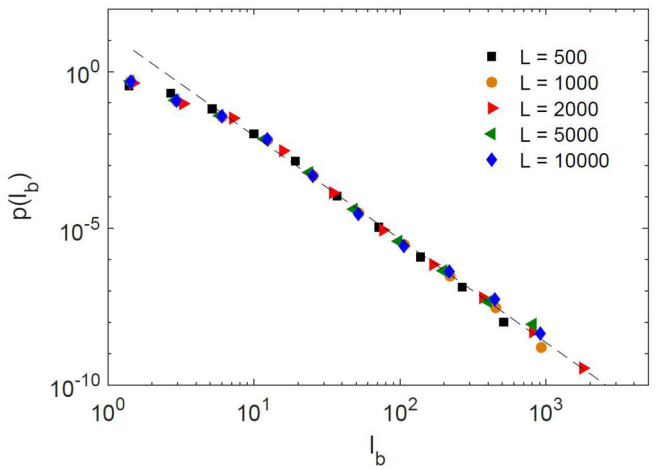

FIG. 4. Probability distribution of the segment lengths $p(l_b)$ for different lattice sizes. The dashed line indicates a power-law fit with exponent $\epsilon = 3.3 \pm 0.1$.

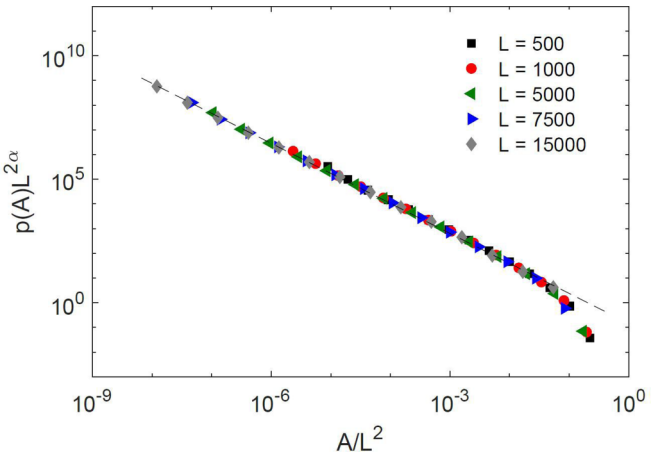

FIG. 5. Data collapse for the probability distribution functions of the areas enclosed by the shortest path and its next shortest alternative $p(A)$ for different lattice sizes L. The dashed line indicates a power-law fit with exponent $\alpha = 1.186 \pm 0.008$.

in length stay the same and hence the two successive sites belong to the same segment. We measure the lengths of these segments l_b and obtain them in a spatially ordered sequence from the top to the bottom of the network along the shortest path. By calculating the sample autocorrelation function of the spatial sequence of segment lengths, we find that the series is uncorrelated, meaning that the length of one segment is independent of the length of the previous one. We present the distribution of the segment lengths in Fig. 4.

The probability distribution of l_b follows a power law with an estimated exponent of $\epsilon = 3.3 \pm 0.1$. Hence, the probability of finding longer constant segments decreases rapidly.

V. ENCLOSED AREA

Next, we study the enclosed area between the shortest path and its next shortest alternative. We consider only the well-defined areas surrounded by a closed loop formed by the two paths. Enclosed areas are apparently compact objects and hence we divide the argument of the proposed scaling function by L^2 to collapse the data. We find that the probability distribution function H follows an exponentially truncated power law. Consequently, we propose a scaling law of the form:

$$p(A, L) = L^{-2\alpha} H\left(\frac{A}{L^2}\right). \tag{4}$$

We obtain an excellent data collapse, shown in Fig. 5, which verifies our proposed scaling law with an estimated exponent of $\alpha = 1.186 \pm 0.008$. Our result is consistent with previous findings on a randomly directed square lattice [8] where an exponent of 1.186 ± 0.001 was found and on an artificial landscape where the area between watersheds was investigated [25] where an exponent of 1.16 ± 0.03 was reported.

VI. CONCLUSION

We studied the effect of sequentially blocking each site along the shortest path of a critical two-dimensional site percolation cluster by considering the shortest alternative path. We derived the average distance between the red bonds theoretically and confirmed it with numerical results. We found the lengths between the red bonds to be power-law distributed and presented a scaling law with an exponent $\delta = 1.64 \pm 0.03$. The comparison between the two paths provides us with the difference in their length and the enclosed area between them. We found the size of the smallest enclosed areas A and the differences in length Δl to be power-law distributed with exponents $\alpha = 1.186 \pm 0.008$ and $\beta = 1.38 \pm 0.03$ using MLE and verified our proposed scaling law by collapsing the data. Further, we counted over how many successive blocked sites Δl stays constant and called this quantity l_b. We found the series of spatially ordered segment lengths to be uncorrelated by calculating the sample autocorrelation function. We presented the distribution of l_b, which follows a power law with an estimated exponent $\epsilon = 3.3 \pm 0.1$, using least squares on the log-binned histogram.

Since percolation describes many natural processes like forest fires [7], electrical breakdown [26], or traffic conditions [6], it would be of interest to link the blocking approach to real systems. Also other shortest alternative paths enclosing not only the smallest area but also all possible areas could be investigated.

ACKNOWLEDGMENT

H.J.H. thanks Funcap and CAPES.

[1] M. Porto, S. Havlin, S. Schwarzer, and A. Bunde, Phys. Rev. Lett. **79**, 4060 (1997).

[2] M. Porto, N. Schwartz, S. Havlin, and A. Bunde, Phys. Rev. E **60**, R2448 (1999).

[3] M. Cieplak, A. Maritan, and J. R. Banavar, Phys. Rev. Lett. **72**, 2320 (1994).

[4] M. Cieplak, A. Maritan, and J. R. Banavar, Phys. Rev. Lett. **76**, 3754 (1996).

[5] E. A. Oliveira, K. J. Schrenk, N. A. M. Araújo, H. J. Herrmann, and J. S. Andrade, Jr., Phys. Rev. E **83**, 046113 (2011).

[6] D. Li, B. Fu, Y. Wang, G. Lu, Y. Berezin, H. E. Stanley, and S. Havlin, Proc. Natl. Acad. Sci. USA **112**, 669 (2015).

[7] G. MacKay and N. Jan, J. Phys. A: Math. Gen. **17**, L757 (1984).

[8] F. Hillebrand, M. Luković, and H. J. Herrmann, Phys. Rev. E **98**, 052143 (2018).

[9] K. Christensen and N. R. Moloney, *Complexity and Criticality*, Vol. 1 (Imperial College Press Advanced Physics Texts, London, 2005).

[10] M. E. J. Newman and R. M. Ziff, Phys. Rev. Lett. **85**, 4104 (2000).

[11] H. J. Herrmann, D. C. Hong, and H. E. Stanley, J. Phys. A: Math. Gen. **17**, L261 (1984).

[12] S. Havlin and R. Nossal, J. Phys. A: Math. Gen. **17**, L427 (1984).

[13] P. Grassberger, Math. Biosci. **63**, 157 (1983).

[14] R. Pike and H. E. Stanley, J. Phys. A: Math. Gen. **14**, L169 (1981).

[15] P. Grassberger, J. Phys. A: Math. Gen. **18**, L215 (1985).

[16] H. J. Herrmann and H. E. Stanley, J. Phys. A: Math. Gen. **21**, L829 (1988).

[17] A. Deluca and Á. Corral, Acta Geophys. **61**, 1351 (2013).

[18] E. P. White, B. J. Enquist, and J. L. Green, Ecology **89**, 905 (2008).

[19] J. Alstott, E. Bullmore, and D. Plenz, PloS ONE **9**, e85777 (2014).

[20] Z. Zhou, J. Yang, Y. Deng, and R. M. Ziff, Phys. Rev. E **86**, 061101 (2012).

[21] A. Coniglio, J. Phys. A: Math. Gen. **15**, 3829 (1982).

[22] D. Stauffer and A. Aharony, *Introduction to Percolation Theory* (Taylor & Francis, London, 2014).

[23] J. Cardy, J. Phys. A: Math. Gen. **31**, L105 (1998).

[24] P. Grassberger and W. Nadler, in *Computational Statistical Physics: From Billiards to Monte Carlo* (Springer, Berlin, 2002), p. 169.

[25] E. Fehr, D. Kadau, J. S. Andrade, Jr., and H. J. Herrmann, Phys. Rev. Lett. **106**, 048501 (2011).

[26] L. Niemeyer, L. Pietronero, and H. J. Wiesmann, Phys. Rev. Lett. **52**, 1033 (1984).